Philosophical Magazine A

ISSN: 0141-8610 (Print) 1460-6992 (Online) Journal homepage: https://www.tandfonline.com/loi/tpha20

Mesoscale simulations of particle pinning

M. Miodownik , J. W. Martin & A. Cerezo

To cite this article: M. Miodownik , J. W. Martin & A. Cerezo (1999) Mesoscale simulations of particle pinning, Philosophical Magazine A, 79:1, 203-222, DOI: 10.1080/01418619908214284

To link to this article: https://doi.org/10.1080/01418619908214284

PHILOSOPHICAL MAGAZINE A, 1999, VOL. 79, NO. 1, 203–222

Mesoscale simulations of particle pinning

By M. MIODOWNIK,† J. W. MARTIN,‡ and A. CEREZO‡

† Sandia National Laboratories, PO Box 5800, Mail Stop 1411, Albuquerque. New Mexico 87185, USA
‡ Department of Materials, University of Oxford, Parks Road, Oxford OX1 3PH, England

[*Received 7 August 1997; revised version accepted 25 March 1998*]

ABSTRACT

Despite much debate, there is still little consensus of opinion on the dependence of Zener pinning (the stagnation of grain growth caused by second-phase particles) on the volume fraction. The controversy surrounds attempts to relate the volume fraction of particles to the final pinned grain size. Analytical theories and 3D Monte Carlo simulations are in disagreement and the experimental evidence is inconclusive. In this paper we contribute to the debate by describing mesoscale 3D Monte Carlo simulations of a single boundary moving through an array of particles. It is found that the simulation temperature is a critical variable, and the simulated boundaries possess mobilities independent of driving force only when $kT' \geq 2$. This is explained in terms of a ledge mechanism of migration in which ledge repulsion becomes important when $kT' < 2$. The effect of T' is critical in determining the geometry of the boundary (and hence the pinning force) during particle bypass. When $kT' = 0$, the expected dimple shape is not observed because the boundary is in a non-equilibrium state (due to ledge repulsion) and this is the origin of the strong pinning observed in the simulations. When $kT' \geq 1$, dimples are observed and the pinning force is in good agreement with analytical theory. The implications of this work on the volume fraction dependence of Zener pinning are discussed.

§1. INTRODUCTION

1.1. *Background*

Zener pinning, the stagnation of grain growth caused by second-phase particles, is a challenging problem for the theorist. A detailed theory needs to incorporate the geometry of a real microstructure: inhomogeneous grain structures, particle size distributions, stringers, anisotropic grain boundary mobilities, etc. Inevitably, analytical theories make assumptions about the microstructure, reducing the problem to a much simpler geometry. The validity of these assumptions can only be ratified by comparing the predictions of the theories with experimental data. The problem is that the data are ambiguous, as two data collations, one by Hazzledine and Oldershaw (1990) and the other by Olgard and Evans (1986) have shown.

Recently Monte Carlo models have been applied to a wide variety of domain growth phenomena; these have been reviewed by Anderson (1986) and Ling and Anderson (1992). In particular Monte Carlo simulations of Zener pinning have been carried out by Srolovitz *et al.* (1984), Anderson *et al.* (1989) and Hazzledine and Oldershaw (1990). The results from these simulations are in strong disagreement

with the predictions of analytical theories. The aim of this paper is to shed some light on the origin of these discrepancies.

1.2. *Analytical approaches*

Analytical approaches generally tackle Zener pinning in two stages: firstly by establishing a pinning force per particle and then by estimating the number of particles per boundary, see figure 1. The earliest example of such an approach is by Zener, as quoted by Smith (1948). When a boundary bypasses a particle, the particle exerts a force of $2\pi r\gamma \sin\theta \cos\theta$ on the boundary (figure 1). The maximum value of this force, F_p, is defined as the pinning force per particle and is given when $\theta = \pi/4$, by

$$F_p = \pi r\gamma, \tag{1}$$

where r is the radius of the particle and γ is the surface tension of the boundary.

Zener estimated the number of particles per area of grain boundary, N_s, by considering the particles to be distributed randomly on the boundary, therefore

$$N_s = \frac{3f}{4\pi r^2}. \tag{2}$$

Combining this with equation (1) gives the pinning stress:

$$\sigma_Z = \frac{3f\gamma}{4r}. \tag{3}$$

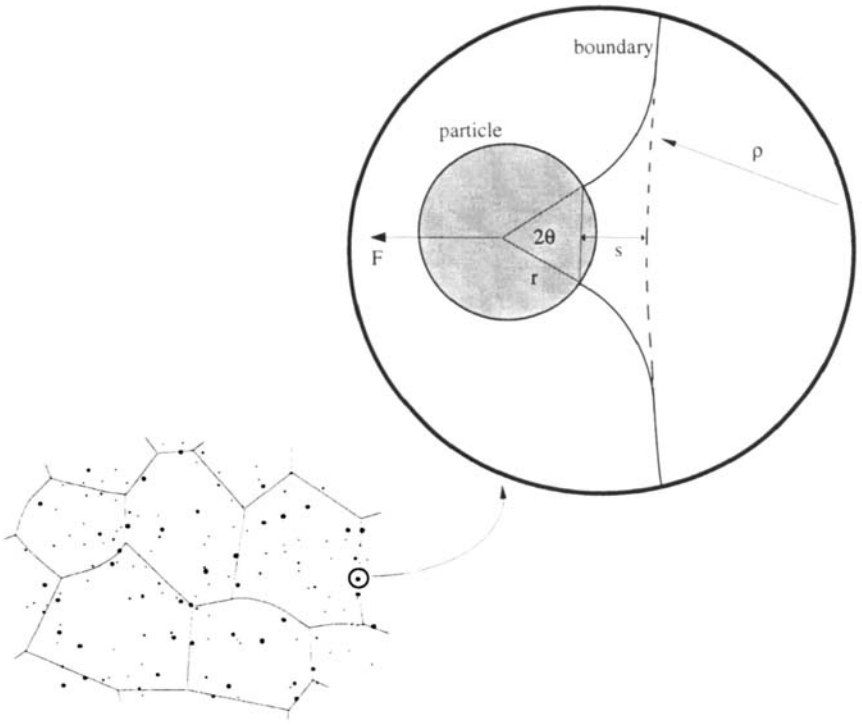

Figure 1. Dimple geometry of particle bypass during grain growth.

Clearly this is a rough estimate. The boundary is deformed near the particle because of surface tension considerations (see figure 1). This shape is often referred to as a 'dimple'. Its profile has been calculated by Hellman and Hillert (1975) and Hazzledine *et al.* (1980) who showed that boundaries remain in contact with particles even when the mean boundary position is more than a distance r past the particle. This implies that the number of particles in contact with a boundary will not be random as assumed by Zener. Hellman and Hillert (1975) incorporated this effect by considering a boundary moving through an array as a multi-dimpled entity. All particles in contact with the boundary and trailing its mean position exert a pinning force on the boundary; similarly particles in front of the boundary tend to pull the boundary forward. If it is assumed that the effects of the particles in front and behind the boundary, whose centres lie within r of the boundary exactly cancel out, then the net pinning stress is due to particles whose centres lie further than r from the boundary. Louat (1982), on this reasoning, gives the pinning function as:

$$\sigma = \beta\sigma_Z \tag{4}$$

where σ_Z is the Zener stress (equation (3)) and β is a function of ρ/r (ρ is the boundary curvature). The estimates of β range from 0 to 2 for values of ρ/r between 1 and 10^5 and illustrate that under most conditions the Zener estimate ($\beta = 1$) remains acceptable.

In practice we are interested in an estimate of the limiting grain size. This is calculated by equating the pinning stress (equation (4)) with the driving force for grain growth, γ/ρ, and assuming ρ is equal to the average grain size D. Thus the pinned grain size is given by:

$$D_c = \frac{4r}{3\beta f^n}, \tag{5}$$

where n is the volume fraction dependence.

1.3. *The importance of dimples*

The value of n (equation (5)) is where the controversy lies: most analytical theories give $n = 1$. Although a number of authors have suggested that n is a function of volume fraction, Hillert (1988), Hazzledine and Oldershaw (1990) and Humphreys and Hatherly (1995) have suggested that $n = 1$ for small volume fractions and $n = 0.33$ for high volume fractions. Three-dimensional (3D) Monte Carlo simulations (Anderson *et al.* 1989, and Hazzledine and Oldershaw 1990) find $n = 0.31$. There is no definitive experimental value for n. There is, however, experimental evidence concerning the pinning force due to each particle. As discussed above, this force depends on the shape of the boundary as it bypasses the particle—the dimple shape. Ashby *et al.* (1969) have examined the dimple formation of soap films bypassing glass balls and water/kerosene interfaces bypassing copper spheres. Ringer *et al.* (1991) used a similar method. The experimental evidence of both papers found good agreement with calculated dimple shapes. In addition there have been experimental observations of dimples in metals and ceramics. For example, the shape of dimples in an Al–Cu alloy has been measured and found to be in agreement with the theoretical analysis (Ashby *et al.* 1969). There is thus good agreement between theory and experiment on the question of dimple formation and particle pinning and this is firm ground on which to test the Monte Carlo

model. The central issue we address in this paper is whether dimples are formed in Monte Carlo simulations.

§2. The model

The mechanism for boundary movement in the Monte Carlo model is the movement of steps on the boundary, which have a height of one site. If particles with a volume of one site are incorporated into the model then it is impossible to detect the presence of dimples around particles because there is insufficient resolution to define the boundary shape during bypass. In this paper we describe Monte Carlo model simulations of Zener pinning with particle sizes $d > 1$ lattice unit (lattice units are used through the paper).

Increasing the size of the model to accommodate larger particles is not straightforward because the computing time scales with the square of the grain size. There is also a kinetic effect; boundary velocities are inversely proportional to boundary curvature, so by increasing the size of the grains we decrease the rate of microstructural evolution. This paper represents a novel approach to this fundamental problem of ever-decreasing returns. Instead of modelling the evolution of a grain structure, we model a single boundary moving through an array of particles. This constitutes a scaling up of the model without the penalties associated with modelling the whole microstructure.

The Monte Carlo Potts model for the simulation of normal grain growth has been described in detail by a number of authors (Anderson *et al.* 1984, Godfrey and Martin 1995). A continuum microstructure is mapped onto a 3D simple cubic lattice of variable dimensions $N_x \times N_y \times N_z$. Each lattice site is allocated a spin number so that all sites within a grain have the same spin. The grain boundaries are represented by the sites which have nearest neighbours of more than one spin. The total system energy is specified by the Potts Hamiltonian:

$$H = E_0 \sum_{i=1}^{N} \sum_{j=1}^{k_s} 1 - \delta(s_i, s_j), \tag{6}$$

where E_0 is a positive constant defining the energy scale of the simulation, s_i is the orientation (spin) of site i, δ is the Kronecker delta function, and the summation is taken over the k_s sites within the neighbour shell of site i and for all N lattice sites.

Domain growth kinetics were simulated with Glauber dynamics using first, second and third nearest neighbours: a site is selected randomly, allocated a new spin number and the change in energy calculated. The probability $P(\Delta E)$ that the site will change orientation is then calculated from the transition probability function:

$$P(\Delta E) = \begin{cases} 1 & (\Delta E \leq 0) \\ \exp(-\Delta E/kT') & (\Delta E > 0) \end{cases} \tag{7}$$

where T' is the simulation temperature and k is Boltzmann's constant. Thus the proposed spin change is always accepted if it lowers the local energy of the site. If it increases the local energy it is accepted according to an Arrenhius probability. The algorithm tends to minimize local interfacial area, which in a polycrystal array leads to grain growth by the movement of kinks or ledges along the grain boundaries.

T' has no physical meaning and must not be construed as being equivalent to a real temperature. It simply alters the transition probability function (equation (7)). Using $T' = 0$ ensures that only events that lower the local interfacial energy of the

system are allowed. Using $T' \neq 0$ allows some events that do not lower the energy. T_c' is the upper limit for T', a critical value for which all site flips become equally probable, and the lattice spins become randomized.

Potts model simulations of grain growth are typically carried out under conditions where $T' = 0$ (Anderson *et al.* 1984, Srolovitz *et al.* 1985, Rollett *et al.* 1988). It is not clear why this should be, except that simulations using $T' = 0$ appear to be successful in simulating the kinetics of grain growth. No systematic investigation of the effect of using $T' \neq 0$ on grain growth kinetics has been performed. The effect of temperature on the kinetics of two-dimensional (2D) domain growth has been reported by Holm *et al.* (1991) and Grest *et al.* (1984). Thompson *et al.* (1996) have reported the effect of temperature on 2D Zener pinning.

The model used in this study is not strictly a Potts model since it only selects boundary sites for spin flips. This serves two purposes. It makes the model more physically significant when $T' \neq 0$, since it does not allow nucleation of new subgrains within grain interiors. Secondly, as the scale of the model increases and the ratio of boundary sites to interior sites decreases, the algorithm becomes more efficient. The definition of the time increment, Δt, corresponding to a single flip attempt was calculated by (Hassold and Holm 1993):

$$\Delta t = 1/\text{Number of boundary sites.} \tag{8}$$

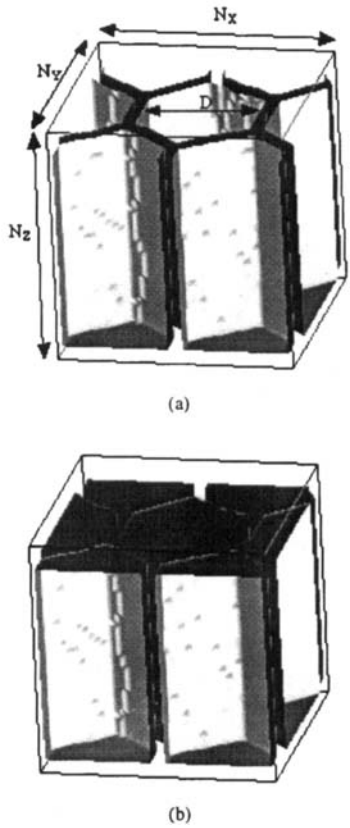

Figure 2. The construction of the initial geometry to simulate the migration of a boundary moving under a constant driving force: (*a*) the vertical network of hexagonal grain boundaries. (*b*) the network after insertion of the planar grain.

The model is therefore identical to the classical Potts model when $T' = 0$ because in both models it is only boundary sites which have a finite chance of being reoriented. The model differs from the Potts model when $T' \neq 0$ because it ignores the interior sites even though they have a finite chance of being reoriented.

A novel geometry was used to simulate the kinetics of a boundary moving under a constant driving force. This geometry consists of a planar grain on top of a hexagonal boundary network and is shown in figures 2 (*a*) and (*b*). The hexagonal boundary network is static throughout the simulation since all the boundaries intersect at 120° and there is no boundary curvature. The planar grain is placed on top of the hexagonal columnar grains as shown in figure 2 (*b*). Only the boundary between the planar grain and the hexagonal grains is in a non-equilibrium state which causes the planar grain to migrate, see figure 3. Boundary conditions are continuous in the x and y directions.

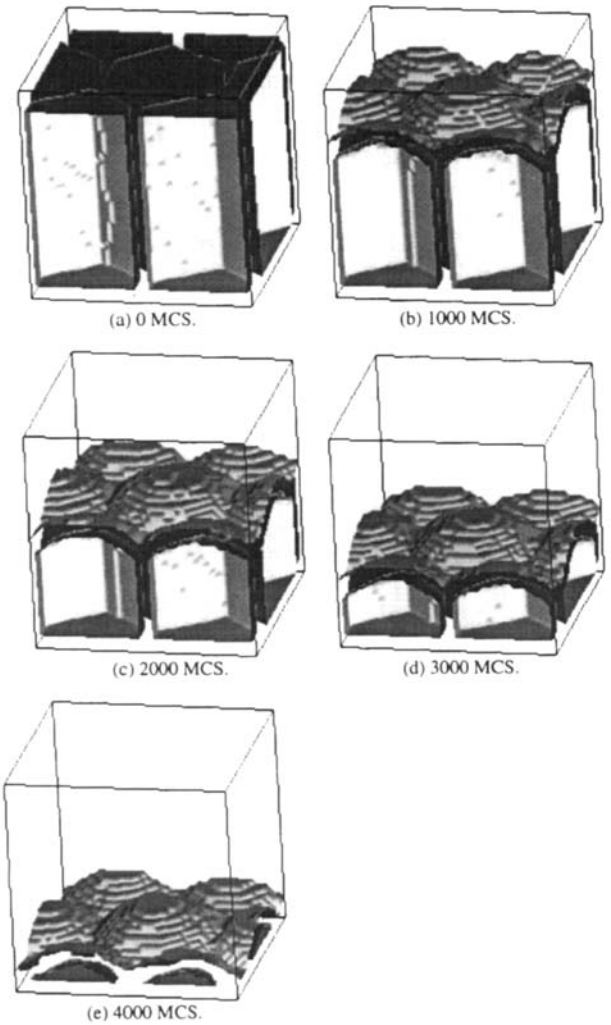

Figure 3. A sequence of snap shots of a boundary migrating under the action of a constant driving force. The simulation was carried out using $D = 25$ and $kT' = 0$ in a simulation volume of $58 \times 50 \times 50$ (in lattice units).

The driving force is provided by consumption of the hexagonal grains by the planar grain. Since the geometry of the hexagonal grains is static, this driving force is constant. The magnitude of the driving force is determined by the size of the hexagonal grains, characterized by the variable D (in lattice units), see figure 2(*a*). For each value of D the N_x and N_y dimensions of the simulation box must be varied to preserve hexagonal geometry. The values of D and their corresponding lattice volumes (in parentheses) are; 5 ($10 \times 12 \times 50$), 10 ($20 \times 22 \times 50$), 17 ($39 \times 34 \times 50$), 25 ($58 \times 50 \times 50$), 50 ($116 \times 100 \times 50$).

§3. Results

3.1. *Boundary velocity*

The boundary adopts an equilibrium shape during migration and then maintains this as it migrates in the z direction, as shown in figure 3. Since the boundary retains its shape, a unique velocity can be calculated. Figure 4 shows plots of boundary velocity for various driving forces. The start and the finish of the migration are nonlinear. The former is due to the initial change in shape of the migrating boundary from a planar geometry to a series of caps. The latter is due to interference as the boundary reaches the extent of the modelling volume. However, for each driving force the boundary moves with a constant velocity between $z = 10$ and $z = 35$. The question of boundary mobility is addressed in §4.

3.2. *Particle pinning*

A regular array of particles lying in the x–y plane was introduced, so that each boundary cap meets a single particle, see figure 5. Each simulation was continued until either the boundary became pinned or reached the limit of the modelling volume. Simulations were carried out with $D = 100$ for a range of particle diameters d and values of kT'.

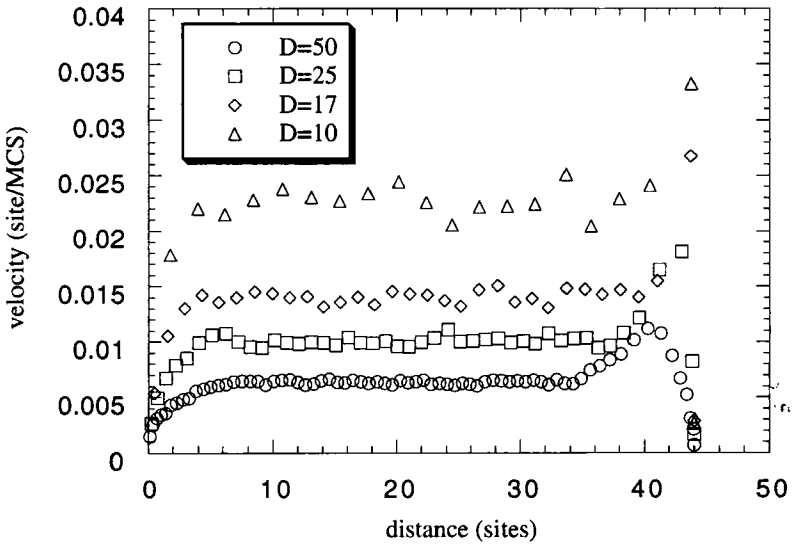

Figure 4. Plot of boundary velocity as a function of the boundary position. Errors are comparable with symbol size.

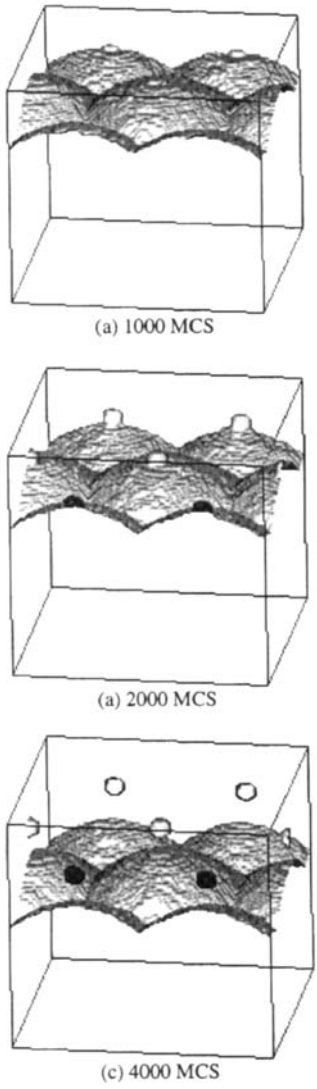

Figure 5. A boundary migrating through a particle array so that each particle interacts with one boundary cap ($D = 50$, $kT' = 1$, $d = 8$).

3.2.1. *The effect of* $kT' = 0$

Figure 6 shows the bypass sequence for a particle of diameter $d = 3$. When the boundary first meets the particle its macroscopic shape is unaffected. As it bypasses the particle it appears to show the formation of a dimple (figure 6(*b*)). However, the beginnings of the formation of facets are evident as the migration continues, see figure 6(*c*). Despite the macroscopic distortion, the boundary bypasses the particle by a mechanism other than dimple formation, see figure 6(*d*). This is the only particle size which allows particle bypass, all particles of diameter larger than $d = 3$ pin the boundary. This pinning event is illustrated in figure 7 for a particle of diameter $d = 8$. The sequence is similar to that when $d = 3$, however after the boundary is faceted no further migration occurs and the boundary is pinned.

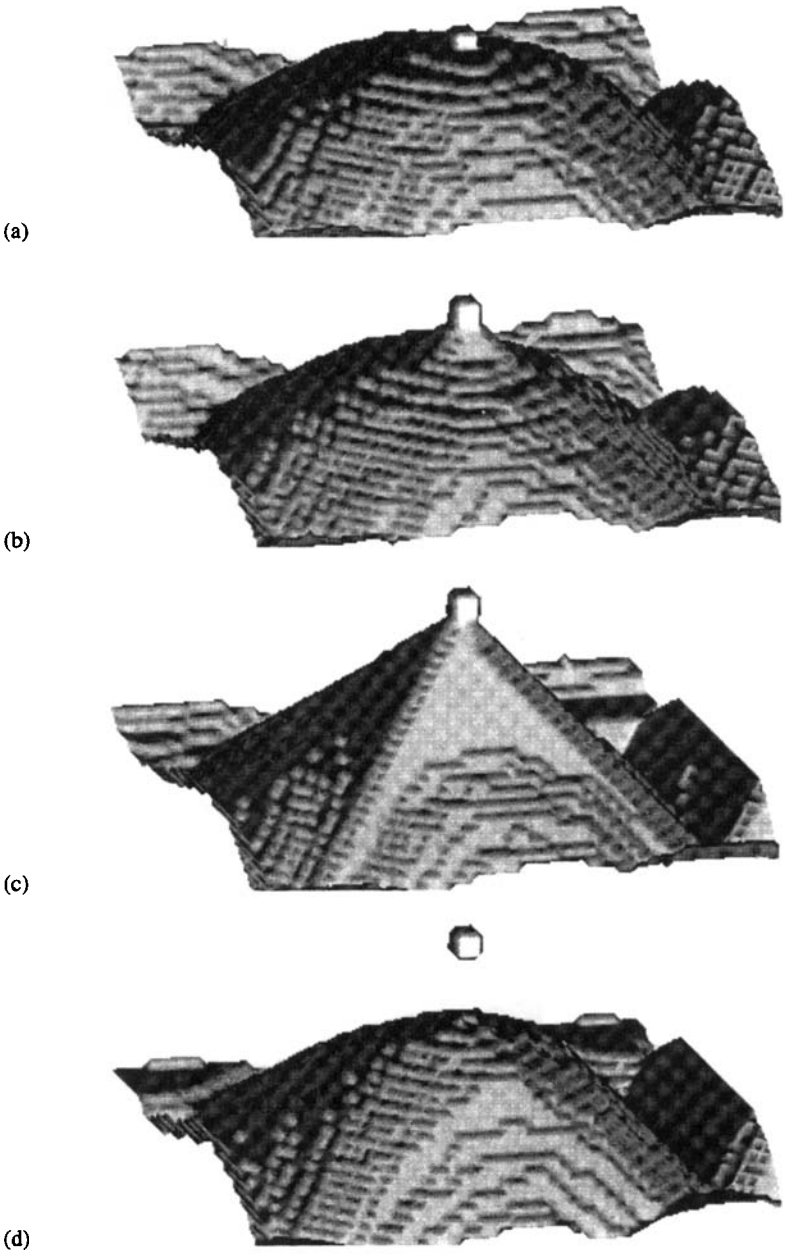

Figure 6. The boundary–particle interaction ($d = 2$, $D = 50$, $kT' = 0$).

3.2.2. *The effect of* $kT' \neq 0$

Simulations were carried out at $kT' = 0.5$, 1.0, 2.0, 3.0 for particles of diameter $d = 8$. When $kT' = 0.5$ the boundary behaves as in the $kT' = 0$ simulation (see figure 8), in that the early formation of a dimple-like entity is the precursor to loss of macroscopic curvature. The loss of curvature leads to the formation of a boundary cone. The tip of this cone meets the particle, resembling a clown's hat, see figure 8 (*c*). Particle bypass is facilitated by a mechanism of narrowing of the tip. However,

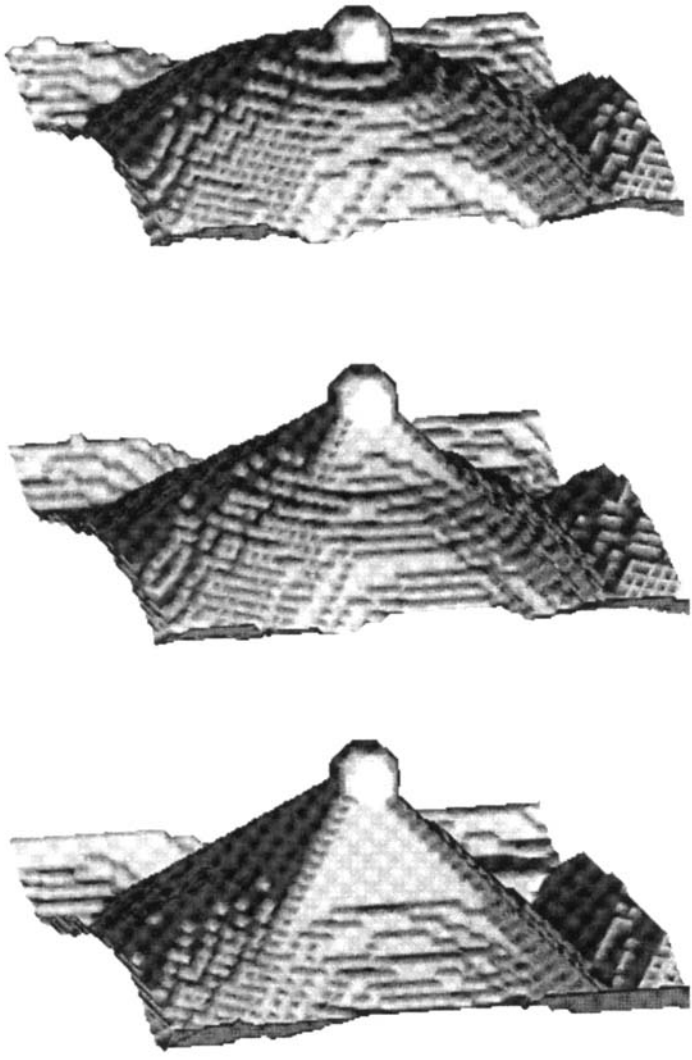

Figure 7. The boundary–particle interaction ($d = 8$, $D = 50$, $kT' = 0$)

dimple formation is the method of bypass for $kT' \geq 0.5$. Figure 9 shows the formation of a dimple when $kT' = 1$; the key property is that it remains a local perturbation on the boundary. The macroscopic boundary curvature is unaffected during bypass. Further increases in kT' do not alter the bypass boundary shape, but merely increase boundary roughness (figure 10).

§4. Discussion

4.1. *Boundary mobility*

Using $kT' = 0$ reduces the complexity of the Potts model to a simple rule governing site reorientation. Namely, reorientation is only allowed when it reduces the local boundary energy. Therefore when $kT' = 0$, the model becomes a method of random minimization of local interface enthalpy. This minimization can be closely

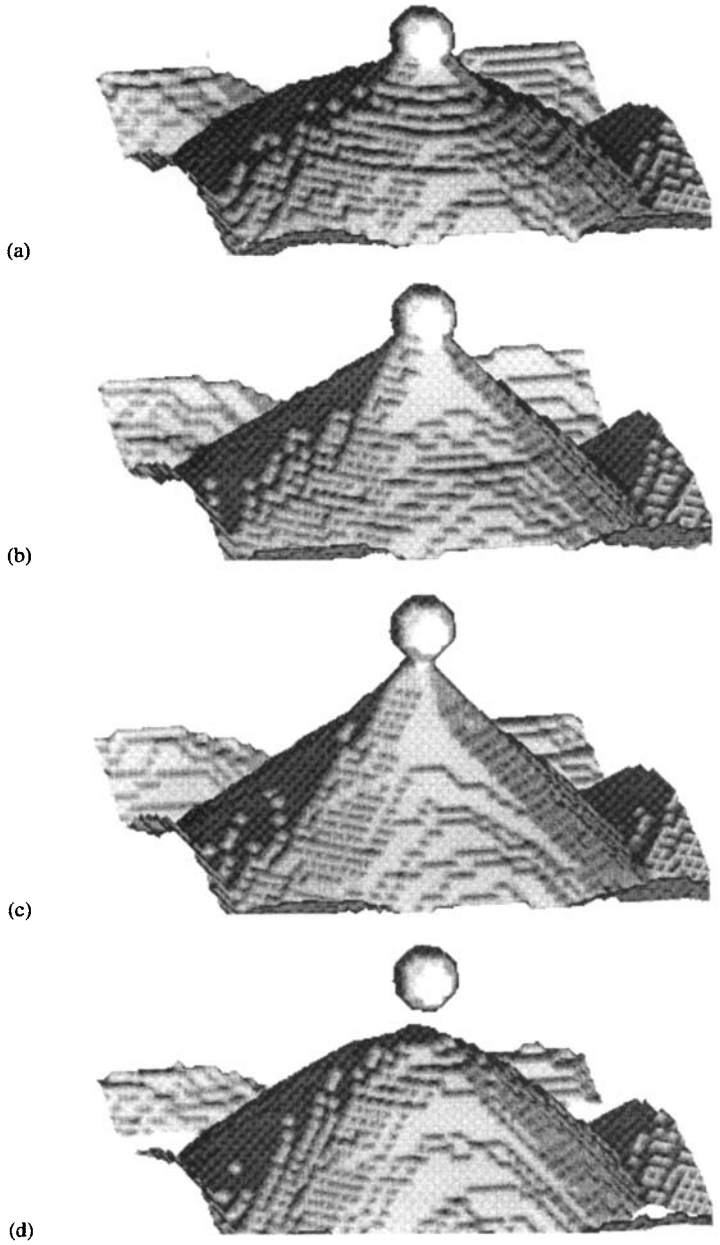

Figure 8. The boundary–particle interaction ($d = 8$, $D = 50$, $kT' = 0.5$).

linked to the thermodynamic explanation of grain growth, where the driving force arises similarly from a reduction in grain boundary area. This does not explain why Monte Carlo models are able to simulate the kinetics of grain growth. Anderson (1986) attributed the success of the model to its boundary migration mechanism: the movement along the boundary of steps in two dimensions and ledges in three dimensions. This is illustrated in figure 11 (*a*) which shows a curved 2D boundary. The boundary moves by the orthogonal movement of steps such as those shown which can move either to the left or the right. If these steps move via a random walk

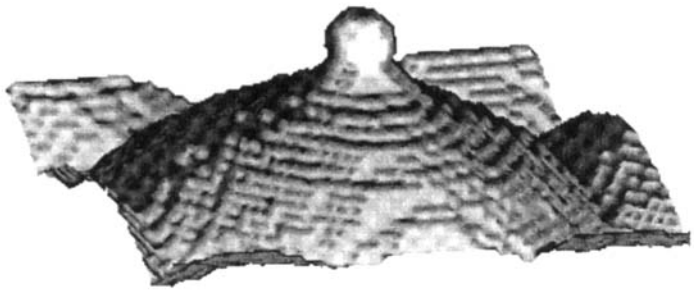

(a)

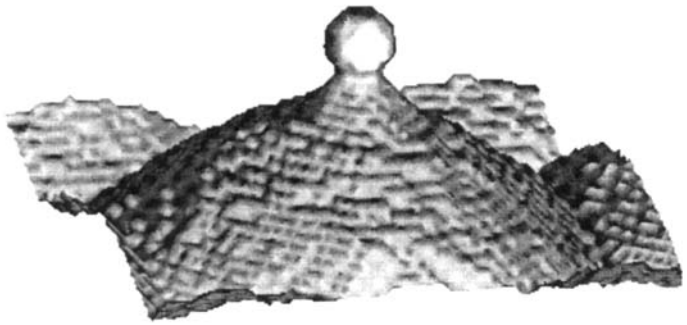

(b)

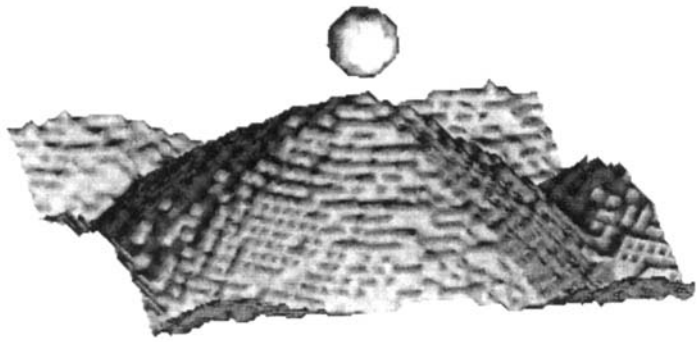

(c)

Figure 9. The boundary–particle interaction ($d = 8$, $D = 50$, $kT' = 1$).

process, the interface mobility will be independent of driving force. This was illustrated by Chen (1987) who used this as the basis for a stochastic theory of grain growth and showed that the random walk of 2D boundary steps or 3D ledges results in the drift of the grain size distribution to larger sizes. This is similar to a kinetic model of grain growth proposed by Louat (1974).

In the current work the driving force acting on each boundary is well characterized and so it is possible to test directly whether the ledge migration mechanism leads to boundary mobilities independent of the driving force. The driving force is given by the rate of consumption of the hexagonal lattice by the moving boundary. This is a function of D and is calculated as follows:

$$F_a = \frac{dA/dz}{dV/dz}\gamma = \frac{16/3^{1/2}D}{8D^2/3^{1/2}}\gamma = \frac{2\gamma}{D}, \tag{9}$$

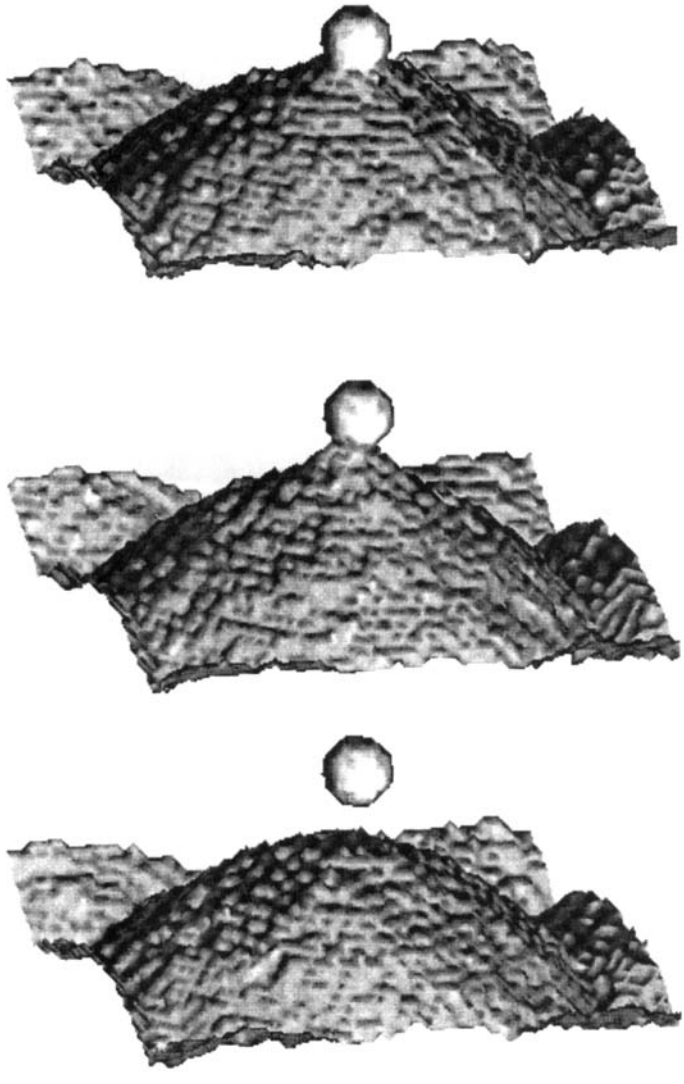

Figure 10. The boundary–particle interaction ($d = 8$, $D = 50$, $kT' = 2$).

where A is the boundary area of the hexagonal grains and V is the volume. (Note that this is identical to the driving force due to a curved boundary with $\rho = D/2$.) Assuming the velocity is proportional to F_d gives:

$$v = \mu F_d = \frac{2\gamma\mu}{D}, \tag{10}$$

where μ is the boundary mobility.

A plot of v versus $1/D$ for $kT' = 0$, 1, 2 is shown in figure 12. The boundary mobility of the model is independent of driving force, in agreement with equation (10), when $kT' = 2$. When $kT' < 2$ the boundaries have constant mobility except when D is smaller than $D_T = 10$ sites, at which point a mobility transition occurs. This is not a quirk of the particular geometry of the current model but is observed in

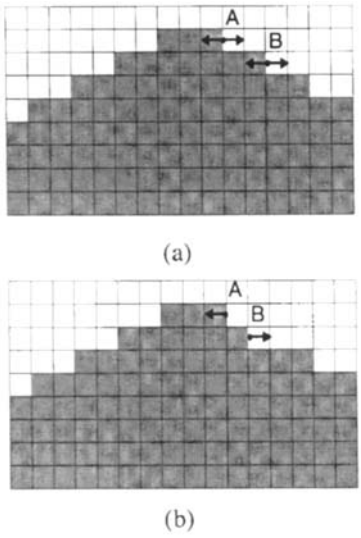

Figure 11. (*a*) An illustration of the boundary migration mechanism in the 2D Potts model. (*b*) An example of ledge repulsion.

many other Monte Carlo studies of grain growth carried out at $kT' < 2$. Anderson *et al.* (1984) studied 2D ($kT' = 0$) grain growth kinetics using a triangular lattice and report a change in growth exponent from short times to long times. This change in kinetics occurs when the average grain diameter is $D_T = 6.3$. Subsequently, in a 3D simulation of grain growth ($kT' = 0$), Anderson *et al.* (1985) reported a transition at

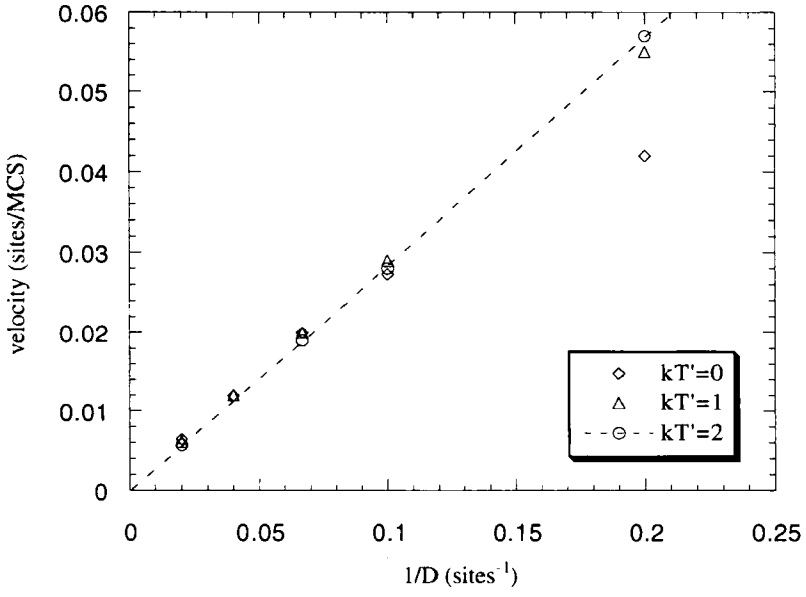

Figure 12. A plot of boundary velocity versus $1/D$. The data are averaged over five simulations, each with a boundary travelling a distance of 35 unit sites. Errors are comparable with symbol size.

$D_T = 5$ sites, and Godfrey and Martin (1995) report a transition in a 2D ($kT' = 0$) model at $D_T = 10$ sites. The effect is likely to be due to 'lattice pinning', which occurs progressively as boundary curvatures approach the lattice size. In particular triple point angles become non-equilibrium because even by using first, second and third nearest neighbours, boundary energy anisotropy exists due to the cubic nature of the lattice. The facets formed during particle bypass (figures 6 and 7) are a good example of the existence of low energy planes. The effect of using values of $kT' > 0$ is to reduce the influence of this anisotropy on the kinetics, allowing a mobility independent of driving force.

When $kT' = 1$ the high curvature boundaries $D < 10$, are hardly affected by the anisotropy and the boundary mobility is only slightly nonlinear, see figure 12. When $kT' = 2$ the boundaries have a constant mobility independent of curvature. From this result it is expected that growth exponent transitions can be eliminated from grain growth simulations if they are carried out a value of kT' which is above critical value. In the current model, this critical value is $kT' = 2$, but it is expected that this value will be a function of simulation variables such as the dimension and type of simulation lattice.

One other consequence of the discrete nature of the lattice should be noted: ledge movement is only random when the ledges are separated from each other by more than one site. Consider the situation when the two steps approach each other, see figure 11 (*b*). If their motion was truly random, step A would now have an equal probability of moving to left or the right. However if we calculate the probabilities for these events we find that when $kT' = 0$, step A has a zero probability of moving to the right, $p(\text{right}) = 0$, and a probability of a half of moving to the left, $p(\text{left}) = 0.5$. Similarly for step B $p(\text{left}) = 0.0$ but $p(\text{right}) = 0.5$. In other words, the steps of like sign repel each other. This effect is also present in 3D systems where ledges of like sign repel each other. For the most part this does not have a dramatic effect on the kinetics, unless the top ledge becomes pinned, as we shall see in the next section.

4.2. *The pinning force*

Figure 13 shows a plot of the change in interfacial energy as the boundary in figure 9 bypasses the particle. The interfacial energy decreases continually indicating that there is always a net force acting on the boundary given by the gradient of the plot. The gradient is modified when the boundary comes into contact with the particle, due to the force exerted by the particle on the boundary. The pinning force can be directly measured from the plot. To compare this force with the theoretical pinning force it must be normalized and so we require a value for γ. This is calculated using a virtual work argument: the boundary moving through a distance of 50 lattice units consumes the boundary sites of the hexagonal vertical boundaries. The boundary area consumed is calculated from figure 2 (*a*) and is $(50.16D/3^{1/2})$ units^2. For $D = 100$, the measured reduction in energy is 182 090 E_0, giving $\gamma = 8.04$ E_0/units^2. Using this value, the measured pinning force is plotted in figure 14 for $kT' = 1$, 2, and 3.

The force exerted by a particle on a boundary has been treated by a number of authors (Hellman and Hillert 1975, Louat 1982, Worner *et al.* 1986). There is agreement as to the shape of the boundary as it bypasses a particle, namely that of a

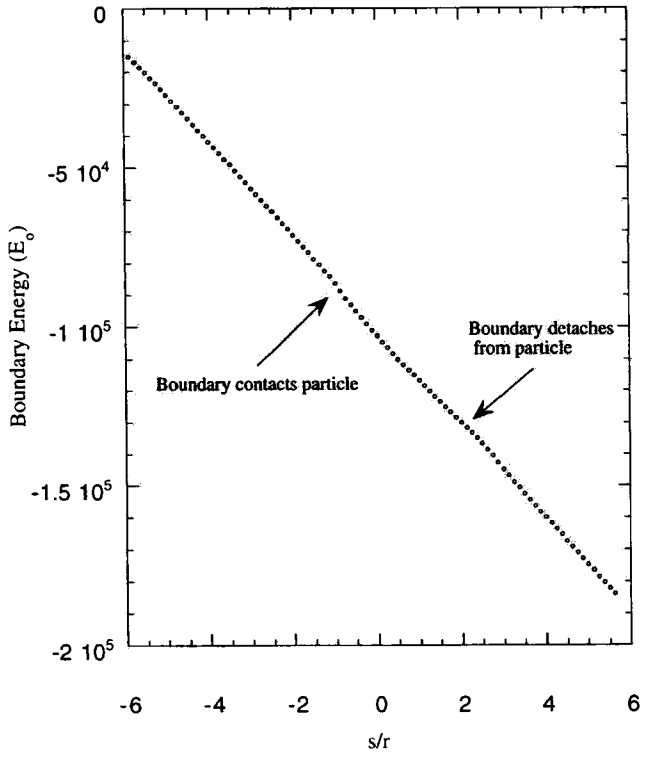

Figure 13. Interface energy as a function of the normalized distance from the particle ($d = 8$, $D = 50$, $kT' = 1$).

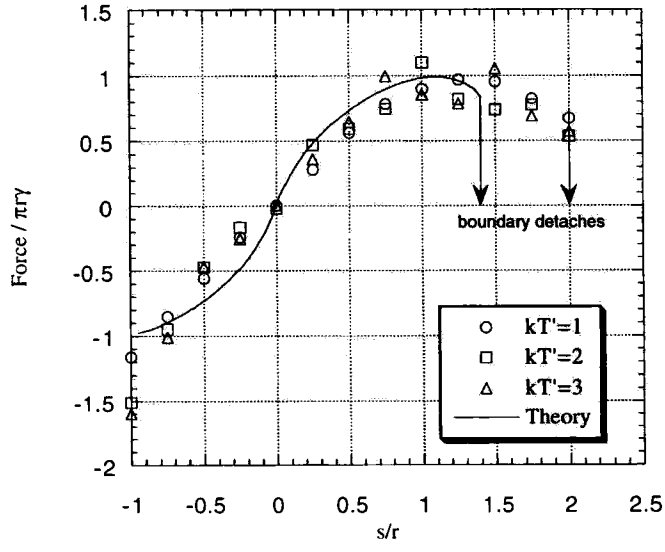

Figure 14. A comparison of the theoretical pinning force (full curve) and the measured pinning forces for $kT' = 1, 2, 3$.

catenoid of revolution. From this, Hellman and Hillert derived an expression for the position, s, of the undisturbed boundary (see figure 1). This is as follows:

$$s = a\left[b + \cos^{-1} h\left(\frac{\rho}{a}\right)^{1/2} - \frac{\rho}{a}\left(1 - \left(1 - \frac{a}{\rho}\right)^{1/2}\right)\right], \tag{11}$$

where $a = r \sin\theta \cos\theta$, $b = \sec\theta - \cosh^{-1}(\operatorname{cosec}\theta)$ and ρ is the radius of curvature of the boundary. Since the force acting on the particle is given by the expression:

$$F = 2\pi\gamma r \cos\theta \sin\theta, \tag{12}$$

the shape of the force/displacement curve can be plotted. This is shown in figure 14. The measured and theoretical pinning curves show good agreement. In particular the maximum forces exerted by the particle on the boundary correspond to those predicted by theory. However, boundary detachment from the particle occurs later than expected at $s/r = 2$ rather than $s/r = 1.4$ which is predicted by theory. This discrepancy is likely to arise from the precise geometry of the particle which, because of the discrete nature of lattice, is cuboid rather than spherical.

4.3. *The effect of temperature*

The measured pinning forces for $kT' = 1, 2, 3$ are shown in figure 14. These show that the pinning force is not a function of kT' (as long as $kT' > 1$). This is an interesting result and can be explained with reference to the mechanism of boundary migration in the model.

First we will consider why the boundary does not form dimples when $kT' = 0$. Figure 15 shows a 2D migrating boundary about to encounter a particle. Grain 1 is growing down the page at the expense of grains 2, 3 and 4. Boundary migration occurs by the orthogonal movement of steps which annihilate when they meet a step of the opposite sign, e.g. steps A and B in figure 15 (*a*). The triple points provide new steps and the process continues until the boundary meets the particle. For particle bypass the two opposite sign steps A and B shown in figure 15 (*b*) must meet and annihilate each other. However, neither step can approach each other because the particle acts as a static step and repels both steps. Steps A and B become immobile becoming static steps themselves which then repel the steps below them in turn. Consequently these steps become pinned also and so eventually do the ones below them. This progression leads to a pile-up of steps continuing down to the triple point eventually leading to the loss of the boundary curvature, the formation of facets and pinning of the boundary, see figure 15 (*c*).

Although this is a 2D example, similar behaviour is observed in the 3D case as shown in figures 6 and 7. The major difference in the 3D case is that, if the particle is small enough, eventual unpinning of the boundary by a mechanism other than dimple formation is possible. However this does not detract from the central issue which is that *ledge repulsion inherent in the model when* $kT' = 0$ *prevents equilibrium boundary tension being simulated.*

When $kT' \geq 1$ the boundary forms dimples during bypass and the measured pinning force is in agreement with the theory. The effect of $kT' \geq 1$ can thought of in terms of the repulsive force between adjacent kinks. When $kT' \neq 0$, there is a probability that two kinks can move into a position directly below each other. This probability increases with kT', in effect decreasing the repulsive force between adjacent kinks, allowing true random walk behaviour of kinks on boundaries. This is

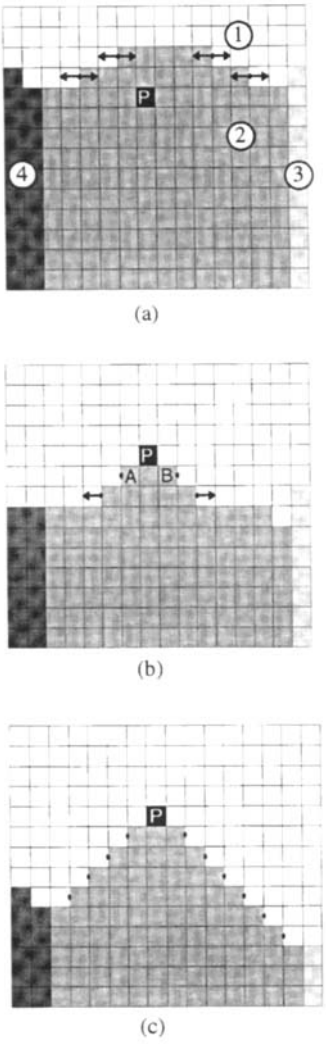

Figure 15. An illustration of strong pinning caused by ledge repulsion in a 2D Potts model simulation carried out as $kT' = 0$.

important because it is the fundamental assumption of stochastic models of grain growth as discussed above. There is a threshold above which the ledge repulsion is reduced to a level where it does not inhibit the kinetics of boundary migration and equilibrium boundary tension is simulated. This threshold occurs at $kT' = 1$ and so further increases in kT' do not affect the geometry of the dimple or the pinning force as shown in figure 14. It is pertinent to ask why the threshold does not occur at $kT' = 2$, a value which we earlier found to be critical in allowing mobilities independent of curvature to be simulated. Inspection of figure 12 shows that the difference between the kinetics of boundaries with $kT' = 1$ and $kT' = 2$ is very small and limited only to boundaries with $D < 5$. The pinning experiments were carried out using boundaries with $D = 50$.

It should reiterated here that T' is not physical temperature. By using non-zero values of T', as we have done in this model, we are not simulating thermal activation

of unpinning. T' is a variable which alters the ledge migration kinetics, it does not change the driving force acting on the boundary.

4.4. *The volume fraction dependence of Zener pinning*

Can we say anything about the volume fraction dependence of Zener pinning? To date all Monte Carlo simulations of Zener pinning reported in the literature have been carried out with $kT' = 0$. We have shown that simulations carried out at $kT' = 0$ exhibit ledge repulsion and therefore the value of n ($= 0.31$) obtained by those models is likely to be due to artificially strong pinning. The Monte Carlo method is capable of simulating pinning correctly as we have shown in this paper and it is expected that simulations of Zener pinning carried out at $kT' = 1$ will provide a more physically accurate test of the analytical models. This will be the subject of a future paper.

§5. Conclusions

A Monte Carlo model of a single boundary migrating under a constant driving force has been developed. The simulated boundaries migrate via a ledge mechanism and show a constant mobility independent of curvature when $kT' = 2$. This is also the case when $kT' = 0$ except for boundaries with high curvature which show low mobility. This is explained in terms of lattice pinning which also gives rise to the phenomenon of ledge repulsion and the formation of facets. We suggest that the change in growth exponent from short to long times in Monte Carlo grain growth simulations, noted by a number of authors, is a result of this lattice pinning and would be eliminated by running the simulations at $kT' \geq 2$.

Dimples are not formed during particle bypass when $kT' = 0$ because of ledge repulsion. The model does not simulate equilibrium boundary tension and so the effective pinning forces are very high. Particles larger than $d = 3$ completely pin the boundaries. When $kT' \geq 1$, dimples are formed during particle bypass and the measured pinning force shows good agreement with that calculated theoretically.

The particle pinning force in Monte Carlo simulations is a function of temperature. To model pinning correctly it is important to make sure that simulations of Zener pinning are carried out with the value of kT' greater than a critical value, in the present simulation this is $kT' \geq 1$.

Acknowledgments

We are grateful to Professor B. Cantor for the laboratory facilities made available to us, and to the Engineering and Physical Science Research Council for financial support.

References

Anderson, M. P., 1986, *Proceedings of the 7th Risø Symposium,* edited by N. Hansen, D. Juul Jensen, T. Leffers and B. Ralph, p. 1.

Anderson, M. P., Grest, G. S., Doherty, R. D., Li, K., and Srolovitz, D. J. 1989 *Scripta Metal.*, **23**, 753.

Anderson, M. P., Grest, G. S., and Srolovitz, D. J. 1985, *Scripta metall.*, **19**, 225.

Anderson, M. P., Srolovitz, D. J., Grest, G. S., and Sahni, P. S., 1984, *Acta metall.*, **32**, 783.

Ashby, M. F., Harper, J., and Lewis, J., 1969, *Metals Trans.*, **245**, 413.

Chen, I., 1987, *Acta Metall.*, **35**, 1723.

Godfrey, A., and Martin, J. W., 1995, *Phil. Mag.* A, **72**, 737.

GREST, G. S., SAFRAN, S. A., and SAHNI, P. S., 1984 *J. Appl. Phys.*, **55**, 2432.
HASSOLD, G. H., and HOLM, E. A., 1993, *Comput. Physics*, **7**, 97.
HAZZLEDINE, P. M., HIRSCH, P. B., and LOUAT, N., 1980, *RISØ International Symposium on Metallurgy and Materials Science*, edited by N, Hansen, A. Jones and T. Leffers p. 159.
HAZZLEDINE, P. M., and OLDERSHAW, R. D. J., 1990, *Phil. Mag.*, A, **61**, 579.
HELLMAN, P., and HILLERT, M., 1975, *Scandinavian J. Metall.*, **4**, 211.
HILLERT, M., 1988, *Acta metall.*, **36**, 3177.
HOLM, E. A., GLAZIER, J. A., SROLOVITZ, D. J., and GREST, G. S., 1991, *Phys. Rev.* A,. **43**, 2662.
HUMPHREYS, F. J., and HATHERLY, M., 1995, *Recrystallisation and Related Annealing Phenomena* (New York: Pergamon), p. 309.
LING, S., and ANDERSON, M. P., 1992, *JOM, TMS*, Sept, p. 30.
LOUAT, N., 1974, *Acta metall.*, **22**, 721.
LOUAT, N., 1982, *Acta metall.*, **30**, 1281.
OLGARD, D. L., and EVANS, B., 1986 *J. Am. Ceram. Soc.*, **69**, C272.
RINGER, S. P., KUZIAK, R .P., and EASTERLING, K. E. 1991, *Mater. Sci. Technol.*, **7**, 193.
ROLLETT, A. D., SROLOVITZ, D. J., and ANDERSON, M. P., 1988, *Acta Metall.*, **37**, 1227.
SMITH, C. S., 1948, *Trans. AIME*, **175**, 15.
SROLOVITZ, D. J., ANDERSON, M. P., SAHNI, P. S., and GREST, G .S., 1984, *Acta metall.*, **32**, 793.
SROLOVITZ, D. J., GREST, G. S., and ANDERSON, M. P,.1985, *Acta Metall.*, **33**, 2233.
THOMPSON, G. S., RICKMAN, J. M., HARMER, M. P., and HOLM, E .A., 1996 *J. Mater. Res.*, **11**, 1520.
WORNER, C. H., CABO, A., and HILLERT, M., 1986, *Scripta metall.*, **20**, 829.